

To Journal of Bridge Engineering, ASCE

CONDITION ASSESSMENT OF SHEAR CONNECTORS IN SLAB-GIRDER BRIDGES VIA VIBRATION MEASUREMENTS

Yong Xia

Assistant Professor,

Department of Civil & Structural Engineering, The Hong Kong Polytechnic University,

Hung Hom, Kowloon, Hong Kong

Tel: (852) 2766 6066; Fax: (852) 2334 6389

ceyxia@polyu.edu.hk

Hong Hao

Professor,

School of Civil & Resource Engineering, The University of Western Australia,

Crawley, WA 6009, Australia

Tel: +61-8-6488 1825; Fax: +61-8-6488 1044

hao@civil.uwa.edu.au

Andrew J. Deeks

Professor,

School of Civil & Resource Engineering, The University of Western Australia,

Crawley, WA 6009, Australia

Tel: +61-8-6488 3093; Fax: +61-8-6488 1044

deeks@civil.uwa.edu.au

Xinqun Zhu

University Research Fellow,

School of Civil & Resource Engineering, The University of Western Australia,

Crawley, WA 6009, Australia

Tel: +61-8-6488 7233; Fax: +61-8-6488 1044

zhu@civil.uwa.edu.au

ABSTRACT

The paper presents a field study on condition assessment of the shear connectors in a full slab-girder bridge via vibration measurements. Firstly, a model updating technique is employed to assess the condition of the whole structure including boundary conditions, bearings, girders, slab and shear connectors from the accelerations on the slab measured in vibration testing. Then, a new damage index based on the difference of frequency response functions on the slab and the corresponding points on the girder is developed to evaluate the condition of shear connectors. The advantage of the new method lies in the fact that it does not need any reference data (undamaged data) for the structure. Compared with the results obtained using the model updating technique, the method is more reliable and accurate in assessing the condition of the shear connectors between the slab and girders. The effect of measurement noise on the damage identification results and the damage quantification are also studied through numerical simulation.

Key Words: shear resistance, concrete slabs, bridge, damage, vibration, uncertainty

BACKGROUND

The precast prestressed deck panel system is very convenient for rehabilitation of deteriorated decks as well as for new bridge construction. This system is widely used in bridges and also long-span buildings. Composite action is achieved by shear connectors between the concrete slab and steel or concrete girders. Obviously the shear strength at the interface between the two interconnected members is of primary importance. During the past years, numerous experimental and theoretical studies have been performed to develop approaches to calculate the shear strength of the connectors, and some of these have been included in design codes (e.g. Australian Standards 2004b). For example, hundreds of push tests have been carried out and used to derive the shear stiffness of stud shear connectors by Oehlers and Coughlan (1986) and Oehlers (1995). Arizumi et al. (1981) studied the shear connectors' elastic and plastic behaviour with finite element methods. A bolted T-stub connection was tested and modelled by Swanson and Leon (2000, 2001).

In aging structures, the condition of shear connectors may not be good due to corrosion and/or overloading. Damage or failure of the shear connectors will reduce the composite action, and therefore reduce the bridge load-carrying capacity. The inaccessibility of the connection system makes direct inspection difficult. On the other hand, the huge number of shear connectors prevents any local non-destructive testing methods to access the connectors one by one. It is of practical importance to develop a new non-destructive assessment technique to detect the integrity of shear connectors. As a matter of fact, examples of condition assessment of shear connectors are very rare in literature. To the authors' best knowledge, only one study has attempted to detect the damage in connectors between steel-concrete composite beams in laboratory (Morassi and Dilena 2003; Dilena and Morassi 2003). In their study, steel studs were used as connectors to link a concrete slab and a steel girder. Different damage configurations in the connectors were induced by saw-cutting one

end connector. Before inducing damage, the concrete surrounding the stud was removed. Then the hole was filled with mortar mixture after saw-cutting. Via vibration methods, an instrumented hammer was used to excite the structure in the undamaged state and in four damaged states of different levels. Modal data such as natural frequencies, modal damping and mode shapes were extracted from the vibration tests. Comparison of modal data found that frequency changes were appreciable, but that mode shapes showed significant changes only for high levels of damage and for high modes.

In Western Australia (WA), about 50 bridges were built in the mid 1970's in the Pilbara region, each based on the same design concepts. The decks of the bridges consist of precast prestressed I-beams supporting a reinforced concrete cast-in-situ slab. Stirrups were embedded in the beams and cast into the slab as shear connectors (or shear links) to join the beams and slab together. After 30 years in service, the shear connectors may have been damaged, as the region has been flooded a few times, or may not suffice to resist the increasing traffic loadings specified in the new design standard. To investigate the integrity of the bridges, and in particular the shear connectors, the Main Roads Western Australia's Bridge No. 852 was chosen for condition assessment through a vibration-based method.

Although many vibration-based methods have been developed in the past few decades, most of applications are based on numerical or laboratory studies (Doebeling et al. 1996; Sohn et al. 2003). The major drawback of these studies, as for most of the current damage detection methods in other applications, is that they heavily rely on a data set (reference data) from the undamaged state or an accurate finite element (FE) model, which is usually not available for aging structures. To overcome this, in the recent years some studies attempted to detect the structural damage without baseline data. Toksoy and Aktan (1994) observed that anomalies in the deflection profile could indicate damage even without a baseline data set. Stubbs and Kim (1996) extended the damage-index

method to structures in which no information for the undamaged structure was available. The modal parameters of the undamaged structure were estimated from the current damaged structure and a corresponding finite-element model. Chen et al (2006) proposed a new indicator based on the transient characteristics of nonlinear vibration. The indicator was directly related to the transient features along the crack surface and no baseline was required. In all these methods, the assessment process is an inverse problem, which reflects into a series of concrete pathologies, such as the non-uniqueness and ill-posedness of the solution. Moreover, there is no method to guarantee a global optimal solution. These issues make many vibration-based methods unreliable for real applications. To investigate the suitability and efficiency of vibration-based methods to assess structural integrity, particularly for shear connectors, a 1:3 scaled bridge model has been built in the structural engineering laboratory at the University of Western Australia (Xia et al. 2006b). The laboratory study shows that the dynamic response of the bridge deck is insensitive to damage in the connector system. This is one of the main difficulties associated with the use of the vibration methods for damage detection, especially for shear connectors.

In this paper, a FE model is built based on the design drawings and field observations. Two methods are used to assess the condition of the shear connectors between the slab and the girders. First the model updating technique is employed to correlate the model prediction with the measurement. The updated model is to evaluate the condition of the connectors as well as conditions of boundaries, bearings, girders and the slab. Similar findings to those reported by Morassi and Dilella (2003) are observed, i.e., although model updating method can detect changes in bridge conditions, only high vibration modes are sensitive to damage in shear connectors. Since high vibration modes of a structure are more difficult to measure accurately, detection of shear connector conditions with high confidence based purely on model updating method is rather difficult. To overcome this difficulty a new damage index based on the difference between the frequency response functions on the slab and at corresponding points on the girders is developed. In

particular, small difference between the measured vibration properties implies the good condition of the connectors, while significant difference indicates some degree of damage in the corresponding connectors. The condition of the shear connectors is evaluated by examining the damage indicator. The primary advantage of the proposed damage index with local vibration measurement is that it does not need any reference data for the structure. In this study, both a model updating method and a local vibration measurement method are used to detect shear connector condition. To enhance the reliability of the results, the effects of measurement noise and the process of damage quantification are also studied.

DESCRIPTION OF THE BRIDGE AND THE FIELD TESTING

Bridge No. 852

The bridge is a continuous three-span structure with an overall length of 53.952 m and width of 9.398 m. The central span of the bridge is 18.288 m long and the external spans are 17.832 m long. The cast-in-situ concrete slab is supported by 7 precast prestressed I-beams in each span, as shown in Figure 1. All the beams are connected at the ends by RC diaphragm beams. The diaphragms are in turn seated on elastomeric bearings placed on RC cap beams over piers and abutments. The shear connectors are 12 mm in diameter and penetrate the RC slab 100 mm before being bent for anchorage. Figure 2 shows a cross section of a beam and a pair of shear connectors. Spacing of the connectors varies from 76 mm in the beam ends to 381 mm in the centre of the beams, as shown in Figure 3.

Theoretical calculations indicate the longitudinal shear capacity is inadequate for the increased vehicle loading and special heavy vehicles, and consideration of strengthening is required (Xia et al. 2006). In addition, the shear connectors may have been damaged, as the region has been flooded many times in the last 30 years. In the region there are a few bridges whose deck was pushed

transversely by the flood or whose approach was rushed away. The objective of the field investigation is to review the condition of the bridge and performance of the shear connections through appropriate methods.

Field testing

The slab of the bridge was tested on 12 October 2005. The measured points are illustrated in Figure 4. In the transverse direction, the accelerometers were placed on the slab corresponding to the centre line of the girders. At the two sides, because the centre of the girders exactly coincides with the edge of the kerbs, the sensors were then placed on the kerbs. In the longitudinal direction 5 accelerometers were placed in each span and one accelerometer at each pier and abutment. This layout results in a measurement grid of 19 by 7. There were 8 sensors roving between 18 sets to cover all 133 points. On the following day, the girders of the bridge were tested. The sensors were installed on the bottom of the girders by climbing up a ladder. Since the clearance height of the central span is higher than 4 meters, it was unsafe to climb up the ladder to place the sensors on the girders in this span. Therefore, the central span was not measured. An instrumented hammer with 12 Lb sledge was used to excite the bridge. A total of 6 hammer blows were applied near to Point A8 in each set. For all the testing on the slab and girders, the impact point (A8) is kept unchanged.

In all the impact cases, 1024 points were recorded with sampling rate of 200 Hz. Based on the measured impact force and acceleration response at individual point, frequency response functions (FRFs) were obtained via signal processing techniques (Ewins 2000).

CONDITION ASSESSMENT OF THE BRIDGE WITH MODEL UPDATING

Most of the vibration-based condition assessments reported in the literature use modal data recorded before and after the onset of damage. As the modal data in the undamaged state of the practical

structure is usually not available, a FE model based on the design is used instead. The model is updated so that the predicted modal properties match those measured as closely as possible. Thus the condition of the bridge can be assessed from the updated model, which represents the current state of the bridge.

Modal Data

The modal properties (natural frequencies, mode shapes and damping ratios) of the structure were extracted by the Rational Fraction Polynomial method (Ewins 2000). In the frequency range 0~30 Hz, 11 modes were identified. Table 1 lists all the frequencies in the range. For brevity, mode shapes are not shown here. Complete results can be found in Xia et al. (2006a).

FE Model

A FE model (denoted as Model 1) based on the original design drawings is created, as shown in Figure 5, to compare with the measured properties of the bridge. Field observations indicated that the two abutments were submerged under soil and rocks. It is assumed that the abutments and the cap beams are unlikely to move. For this reason the abutments and cap beams are removed from the model to reduce the number of elements. The upper structure rests on the bearings on the two abutments. The FE model has 907 elements and 949 nodes each with six degrees of freedom (DOFs). 294 DOFs are constrained, while 5400 DOFs are active in the model. In particular, the piers consist of 32 shell elements, the slab has 288 shell elements at the central axis, the girders have 252 shell elements, the diaphragms have 48 shell elements, the shear connectors are modelled by 231 beam elements, the bearings are modelled by 28 beam elements, and 28 spring elements are used to model the incomplete boundary condition in both ends. In the model, the geometry is based on the design drawings, and has been confirmed by the field measurements. Mechanical parameters (modulus of elasticity, stiffness) are estimated from design drawings, standards and literature as follows.

Modulus of elasticity

According to the Australian Standard (2004a), the modulus of elasticity of concrete is $E_c = 0.043w^{1.5}(f_c)^{0.5}$, where w = density, f_c = compressive strength of concrete. It should be noted that the true value may vary from this estimation by up to $\pm 20\%$. The modulus of elasticity of steel is taken as $E_s = 2 \times 10^5$ MPa.

Boundary conditions

The bridge was designed as being simply supported on the bearings at the two abutments. However, corrosion of bearings often causes additional constraint for both rotations and longitudinal displacements (Eom and Nowak, 2001). In the present model, therefore, the supports at the two abutments are assumed to be partially constrained by applying elastic spring elements to the top and bottom of the girders in the longitudinal direction. These springs partially restrain the bridge from longitudinal displacement and rotation. In practice, the degree of partial constraint (represented by spring stiffness k) can vary from girder to girder, and is structure dependent. Therefore, in this study, the stiffness values of k_{top} and k_{bottom} are first estimated based on the literature (Eom and Nowak, 2001). The values are included in the model updating procedure to identify the actual constraint conditions more accurately. Initial values were taken to be $k_{bottom} = 4 \times 10^8$ N/m and $k_{top} = 2 \times 10^6$ N/m for each girder.

Shear connectors

In the past, many researchers have introduced different methods of modelling shear connectors in composite construction. Oehlers and Coughlan (1986) investigated the behaviour of shear connectors when subjected to both static and cyclic loadings. Studs embedded in strong concrete were found to be stiffer than those in weaker concrete, which indicated a strong relationship between the shear connector behaviour and the concrete compressive strength. Generally, either full

interaction has been assumed or the shear connectors have been treated as rigid or elastic springs. In some circumstances, the connectors have been smeared over the entire interface and the smeared interface has been modelled by special finite elements. Chiewanichakorn et al. (2004) modelled stud shear connectors by three nonlinear springs in the three Cartesian coordinate directions to simulate the shear stiffness of the shear connectors at the steel–concrete interface. The stiffness of the spring normal to the interface is computed as the axial stiffness based on the diameter and embedded length of the shear connectors. Springs representing the resistance to shear force provided by dowel action from the shear connectors are approximated by

$$K_{dwl} = \frac{P_{st}}{d_{sh}(0.16 - 0.0017f_c)} \quad (1)$$

where K_{dwl} = shear stiffness (N/mm); d_{sh} = diameter of the shank of shear connector (mm); and P_{st} = static strength of shear connector (N) computed by

$$P_{st} = 4.3A_{sh}f_u^{0.65}f_c^{0.35}\left(\frac{E_c}{E_s}\right)^{0.40} \quad (2)$$

where A_{sh} = area of the shank of shear connector (mm²); f_u = ultimate tensile strength of shear connector material (MPa). In the present bridge, each connector is made of steel bars of 12.7 mm in diameter. Static strength of each shear connector is calculated as $P_{st} = 43.4$ kN, and shear stiffness as $K_{dwl} = 5.37 \times 10^7$ N/m.

In the studies mentioned above (Oehlers and Coughlan, 1986; and Chiewanichakorn et al. 2004), bending stiffness is not taken into consideration. However, connectors can also resist bending. Including bending stiffness makes the modelling more accurate. In the present study, a connector is modelled as a short beam element which links the slab and girders. The upper node of a connector coincides with the central axis of the slab, which is modelled by shell elements, and the lower node of a connector coincides with the upper joint of the corresponding girder, which is also modelled by

shell elements. The axial stiffness and shear stiffness of a connector are identical to the previous formulae, that is, $K_{axial} = E_s A_{sh} / L$, and $K_{shear} = K_{dwl}$. Bending stiffness of a connector is based on the force equilibrium of a beam element. For a beam in which shear deformation is considered, the stiffness coefficient associated with transverse translation is equivalent to the shear stiffness. The other stiffness coefficients can be developed in a similar way to the elemental stiffness matrix of the traditional beam element (Przemieniecki, 1968).

As there are 81 pairs of shear connectors in each girder (as shown in Figure 3), modelling each one individually will result in a large FE model, and also huge number of elements to be updated, which causes the updating stage to be very time-consuming. Moreover, it is not practical to detect possible damage in one single connector, because removing a single connector will cause little change in the modal properties. From a practical point of view, combining a few connectors as one single “super connector” is a natural and acceptable choice. To verify this simplification, two finite element models (as shown in Figure 6) have been built to examine the effect of this simplification on the modal properties. For simplicity, both models include only the first span of the full structure. In the fine model (Model 2), each pair of connectors is modelled as a single beam element, the mechanical properties of which are calculated based on the above description. The mesh of the connectors in one girder is illustrated in Figure 3. The girders and slab are correspondingly meshed to match those of the connectors. There are 72 connectors in the figure as the 9 in the two ends are merged into the diaphragms. In the simplified model (Model 3), all the material properties are the same as Model 2 but with a different mesh, where groups of connectors are combined as one single “super connector”. Figure 3 also shows the mesh of the “super connectors” in one girder of Model 3. The central “super connector” represents 4~5 real connectors and “super connector” near the ends represents 7~9 real connectors. Comparison verifies that the first 30 global frequencies and mode shapes of the two models agree very well. There are some local modes of the girders in the transverse direction which demonstrate relatively large differences. However, only vertical global

modes are measured and considered in the present study. Therefore the simplified model can be used to adequately represent the real structure.

The model of the whole structure (Model 1) is built in a similar manner to the simplified one-span model (Model 3). Model 1 was first constructed in ANSYS (ANSYS, 2004). Its geometry and elemental information were then passed into a MATLAB (MATLAB, 2005) based software package for modal analysis and model updating.

Model Updating

In order to evaluate the condition of each component of the bridge, especially the shear connectors, nearly all the elements are included in the model updating except the piers. In particular, there are three parameters to update for all the shear connectors and central bearings, that is, axial stiffness (EA), bending rigidity along Y axis (EI_{yy}) and bending rigidity along X axis (EI_{xx}). The orientation of the coordinate system can be found in Figure 5. For the spring elements in the two abutments, the stiffness (k) is updated. For the other elements (diaphragms, girders and slab), only the modulus of elasticity (E) is updated. Updating E is equivalent to changing the elemental axial (EA/L) and bending (EI/L^3) stiffness simultaneously. However, only E is updated as changing geometry (width and height) is much more difficult to program. Therefore, the updated results do not imply the real change in E , but changes in the element stiffness. In total there are 1365 parameters included in the model updating process. It is noted that we update all the parameters independently in stead of grouping some elements. This is to evaluate the condition of the individual elements, especially the shear connectors, rather than assessing the super-elements as usually adopted (Zanardo et al. 2006).

Since there are a large number of parameters to be updated, the state-of-art optimisation algorithm (Trust-Region method) provided by MATLAB based Optimization Toolbox (MATLAB, 2005) is utilised in the optimal model updating process. The algorithm is a specially designed for large-scale

problems, and can deal with thousands of parameters simultaneously. Within each iteration, it can automatically choose the direction and step so that the solution approaches the optimum. The model updating procedure stops when the specified tolerance is achieved or the maximum number of iterations is exceeded. Normally the tolerance is specified on the iteration step and/or the derivatives, which is set to be 10^{-6} in the present study.

The objective function to be minimised is the combined error of frequencies and mode shapes between analysis (denoted as “ A ”) and experiments (denoted as “ E ”) (Hao and Xia, 2002), expressed as follows:

$$J(p) = \sum_{i=1}^{nm} W_{\lambda_i}^2 [\lambda_i(\{p\})^A - \lambda_i^E]^2 + \sum_{i=1}^{nm} W_{\phi_i}^2 \sum_{j=1}^{np} [\phi_{ji}(\{p\})^A - \phi_{ji}^E]^2 \quad (3)$$

where p is a vector of the structural parameters to be updated, λ_i is the i^{th} eigenvalue, $\{\phi_{ji}\}$ are the j^{th} component of the i^{th} mode shape, and W is a weight matrix that is a diagonal positive definite matrix, weighting the contribution of each term. Only the measured np points ($np = 133$ here) and nm modes ($nm = 11$ here) are chosen out of the full set of numerical mode shapes for comparison. The elements of the weight matrix are set to 0.1 for mode shape and 1.0 for frequency as the measured mode shapes is usually less accurate than that of the frequencies by one order (Hao and Xia, 2002). It should be noted that the optimisation methods guarantee neither the uniqueness of the solution nor the global minimum. Therefore the results obtained are not necessarily the best solution. These are the drawbacks of the optimisation based model updating techniques. However, with the very small tolerance of 10^{-6} used in the study, the updated model should reflect some true features of the real bridge structure.

Starting from the initial data ($p = p^0$), the updating process converges with 155 iterations. The modal data of the updated model are compared with those before updating in Table 1. It is clear that the updated model matches the measurements better than the model before updating. In particular, most

frequency differences are less than 5% and the averaged value is 2.4% (12.2% before updating). In addition, most MAC values are greater than 0.90 and the averaged value is 0.91 (0.84 before updating).

The element stiffness parameters of all members of the structure in the updated state are also obtained. Figure 7 shows the damage indicator (DI) of different components. In the present study, DI is defined as parameter change ratio:

$$DI_i = \frac{p_i^u - p_i^0}{p_i^0} \quad (4)$$

where p_i^u is the i -th updated structural parameter and p_i^0 is the i -th initial parameter. If the stiffness parameter of an element is less than the designed value (with a negative DI), the element is believed to be weaker than expected, and possible damage exists. The parameter change ratio indicates the severity of damage. In contrast, if the parameter of an element is larger than the designed value, the element is believed stronger than expected. For brevity, DIs of springs, bearings and diaphragms are not shown here. It is found that the stiffness of the springs generally increases by about 80% ~ 130%, indicating the initial model underestimates the true value. This confirms that the supports are partially constrained, even though they were designed as simply supported. For bearings, the parameters vary for different positions, and the changes are about 100% ~ 200%, possibly due to some additional constraints. For diaphragms, the change is insignificant.

In Figure 7, the shaded bars denote the negative values of DI, while blank bars represent positive DI values. It can be seen that most of DIs in the slab are lower than the designed values by about 60%, showing some degree of deterioration after in service for 30 years. In fact some significant cracks were observed in the slab during the field testing. Excessive loading on the bridge might be one reason, as oversized road trains were observed crossing the bridge every day. The increasing number of oversized vehicles may exceed the original design capacity. DIs of most girder elements

are about 0.2~0.6, implying that the real stiffness of the girders are higher than the initial model. One reason might be due to the inaccuracy in the estimation of E_c . Another one is because the reinforcement bars are not considered in calculation of sectional inertia, which will increase the stiffness by about 10% as $E_s = 5E_c$ and reinforcement is located in the top and bottom of the girder section. The condition of the girders is believed to be good in all instances.

For shear connectors, there is a fair variation in terms of axial rigidity and bending rigidity along X-axis and Y-axis. To evaluate the condition of connectors at different positions, the three DIs of each element are combined by averaging the three values. The results are illustrated in Figure 7. The connectors are further clustered into groups according to their geometric position, that is, left, central and right in each span. The condition of the connectors is then evaluated based on the combined indicators. Due to the structural redundancy and the safety factor employed in the initial design model, shear connector elements with stiffness loss higher than 90% are believed to be in bad condition. Consequently elements with combined indicators less than -0.9 are designated as “Bad”. Similarly the condition of the elements with the combined indicators larger than 0.0 is “Good”, -0.5~0.0 is “Fair” and -0.5~-0.9 is “Poor”. Based on the above definition, the condition of the shear connectors in the bridge based on the global approach is summarized in Figure 8. From the figure, it can be found that most of the connectors are fair while some are poor, especially in the third span. It should be noted that this definition of the shear connector conditions as good or bad is subjective, although it is associated with quantitative stiffness estimations.

CONDITION ASSESSMENT OF SHEAR CONNECTORS WITH A NEW DAMAGE INDEX

METHOD

As the model updating method relies on the initial model developed from design drawings, which inevitably contain errors, a new damage index method is presented here to detect possible damage

in the shear connectors. This approach is based on the fact that when the condition of a shear connector is good, connection of the slab and the girder is adequate, and consequently the response of the slab and the girder is similar. In contrast, when damage has occurred at some connectors, the slab separates from the girder, and the nearby points on the slab may respond differently from those on the girder. Therefore, similar vibration properties between the slab and the girders implies good condition of the connectors, while significant difference indicates some degree of damage in the corresponding connectors. To take advantage of this, sensors were placed on top of the slab to measure response of the slab, and also underneath the corresponding girder to record its response. By proceeding in this way, the need to use the data from the undamaged model is avoided.

Relative difference of FRFs

To quantify the difference in response of the slab and the girders, the relative difference of the FRFs (RDFRF) between the girder and the slab is used to evaluate the condition of the shear connectors.

This is defined as:

$$RDFRF(H_i^G, H_i^S) = \frac{\left\| \{H_i^G\} - \{H_i^S\} \right\|}{\left\| \{H_i^G\} + \{H_i^S\} \right\|} \quad (5)$$

where H_i is the FRF measured at the i^{th} point, superscripts “G” and “S” represent the points on the girder and slab, respectively, $\|\cdot\|$ denotes the Euclidean norm, $|\cdot|$ is the absolute value (or magnitude of the complex number) and $\{\cdot\}$ is the vector of the FRF including all the measured frequency lines (0~100 Hz). A low RDFRF value means a small difference between the response at the point on the slab and the corresponding point underneath the girder, implying a good condition of the connector. On the other hand, a high RDFRF value means a significant difference in the responses at the particular point, which indicates damage in the vicinity.

A laboratory study has found that RDFRFs gave more accurate and consistent shear connector condition detection than the model updating methods (Xia et al. 2006b). That study found that the

RDFRF value is about 0.1 in the undamaged state and 0.4~0.6 in the completely damaged (no shear connector) state. For the prototype bridge, this value may be different, but it is impossible to conduct an experimental study on a prototype bridge for undamaged, partially damaged and completely damaged states. Due to this reason, in the study described here a FE model simulation is employed to quantify the RDFRF corresponding to the various damage states. The model simulation is used to: 1) verify that RDFRF is an indicator sensitive to damage of the shear connectors; 2) investigate the effect of modelling error and measurement noise on the results; 3) give a RDFRF threshold to define damage of the connectors with confidence; and 4) quantify the damage of the connectors in terms of the stiffness loss of the connectors. The results will be then applied to the bridge in question.

FE model simulation

Model 1 described previously is used for the simulation. To simulate the real situation, one of the measured hammer force time histories is applied to the bridge model and the response of the structure is solved by numerical integration. With similar signal processing, FRFs at the measurement points on the slab and girders are derived, and then RDFRFs are calculated using Eq. (5). Figure 9 illustrates the calculated RDFRFs at all the measured 133 points (19 by 7 grid lines) in the undamaged state. The position of the measurement points is illustrated in Figure 4. To simulate the damage in the shear connectors, the stiffness parameters of some connectors are set to zero. As explained previously, it is not practical to detect the damage in one single real connector. It is only practical to detect the damage in a small region. Therefore, the shear connectors in each span are clustered into three groups according to geometric position, namely left, central and right. In the left part, there are four connector elements corresponding to 28 real connectors. In the central part, there are three connector elements corresponding to 10 real connectors. The right part has four connector elements corresponding to 34 real connectors. Figure 9 also shows the RDFRFs in a damaged state in which the shear connectors in the centre of the first span (around Point A4) are removed. This

figure shows that all the RDFRFs in the undamaged state are less than 0.05. In the damaged case, however, RDFRF at A4 increases to 0.46 with little change at other points (although those at nearby points rise slightly). This observation shows that the indicator (RDFRF) is sensitive to the local damage in shear connectors, and not sensitive to the damage away from the point of evaluation.

The above simulation can be applied to all the other points. However, the simulation results with noise free data may give a false indication, as uncertainty is inevitable in practice. To reliably evaluate the condition of the shear connectors, uncertainty should be taken into consideration. In this study uncertainty is assumed to be due mainly to the inaccuracy of the FE model and the noise and errors in the measurements. However, numerical calculation indicates that inaccuracy of the FE model does not affect the RDFRF much, because RDFRF indicates the response difference between the slab and girders. For example, when the modulus of the entire slab decreases by 50%, the largest change in RDFRF is only 0.013. Therefore, only the effect of measurement noise is considered in detail here.

Uncertainty study

As the sensors have been calibrated, the error from the sensor is negligible. The inaccuracy of the measurements mainly comes from: 1) signal noise, and 2) unmeasured ambient excitation (input), both of which are assumed to have the characteristics of random noise. The ambient vibration recorded on the bridge when it is free from traffic and hammer impact is about 0.01 m/s^2 (1% of the maximum response), and the noise of the recorded input force is about 50 N (0.5% of the maximum force). These values are assumed for the level of random noise in the measured accelerations and impact force in order to conduct the numerical investigation. Using Monte Carlo simulation, random noises are added to the input force and the calculated accelerations, and the RDFRFs are then computed. The mean value and standard deviation of the RDFRFs are calculated for all the simulations. In the undamaged case, a convergence study found that 1000 runs of Monte Carlo

simulation were required to get stable values for the mean and standard deviation. Consequently 1000 runs were applied to other situations also. For the undamaged case mean values (μ) of RDFRFs are about 0.12~0.14 and standard deviations (σ) about 0.008~0.025. By assuming that the RDFRFs have normal distribution, a reliable bound of the RDFRF for the undamaged state can be estimated as $\mu + 1.645\sigma$ for the confidence level of 95%. The bound varies according to the position of connectors. For example, the bound with the confidence level of 95% for A4 is about 15%. When RDFRF of A4 is less than the bound, there is believed no damage, otherwise it is believed there is some degree of damage at the connectors around the point.

Clearly RDFRF values are associated with the damage severity. To quantify the damage, the effect of different damage severity is investigated by setting the stiffness loss to different levels. For example, for damage around Point A4, the stiffness loss of the connectors is set to 0%, 50%, 80%, 90% and 100%, respectively, and the mean values and standard deviations of RDFRFs at A1~A7 are computed. the results are illustrated in Figure 10. Here 0% indicates no damage and 100% means complete removal of the connectors.

Condition of shear connectors in the bridge

The above technique was then applied to the measured data for the actual bridge. Figure 11 shows the results of the indicator calculated for the first girder, i.e., Points A1~A7 and A13~A19, according to Eq. (5). Points A8-A12 are not included because the measurement on the girder in the centre span was not performed, due to the reasons discussed in section 2.2. Figure 11 shows that the RDFRFs in the first span are about 0.20 and those in the third span are about 0.30, with the highest value being 0.41 at A17. Based on the simulation results, the connectors in the first girder (the first and third spans) of the bridge have some degree of damage at a confidence level of 95%. To quantify the damage in different connectors, RDFRFs are compared with the simulation results with

different damage severities. For example, comparing Figure 10 and Figure 11, the most likely the stiffness reduction of the connectors at A4 is about 70%.

Using the same approach to the definition of condition as in the Part 3, the stiffness loss higher than 90% is designated as “Bad”, 50%~90% is “Poor”, below 50% is “Fair” and no damage is “Good”. Consequently, the central part of the first girder in the first span is evaluated as “Poor”. Similar analysis finds that the left and right parts of the first girder in the first span are “Poor”. Those of the first girder in the third span are respectively evaluated as “Poor”, “Poor” and “Bad”.

The above procedures were also applied to the other girders. The results are position dependent. It was found through numerical simulation that removing the connectors in the group will cause mean values of RDFRFs increase to 0.4~0.6 with little change in the standard deviations, compared with the undamaged case. For brevity, RDFRF values for other girders are not shown here. The conditions of these connectors were assessed in the same manner, and the results are plotted in Figure 12.

Figure 12 shows that the condition of the connectors in the first span is better than these in the third span. Most of the first span is “Fair”, while the third span is in “Poor” condition with two parts in “Bad” condition. Comparing Figure 12 with Figure 8, the condition of the connectors by the new damage index method is worse than that obtained by the model updating method. This is because the results in Figure 8 have been averaged from three damage indicators. Combining the results from the two figures, it can be concluded with a higher confidence that the shear connectors in the first span and the central span are fair, while those in the third span are not so good.

CONCLUSIONS AND DISCUSSIONS

Two methods have been applied to a slab-girder bridge to assess the condition of the structure, particularly the condition of the shear connectors between the girders and slab. The model updating approach indicated that the condition of the girders and bearings are good, but that the entire slab has some degree of deterioration, and these findings were supported by visual observation. Using a new damage index method which compares the response of the slab and girders, the condition of the shear connectors was also evaluated. Combining the results obtained by the two approaches, it was concluded that most of the shear connectors in the first two spans are in fair condition, but those in the third span are not good.

As the new damage index method does not need baseline data, it is a more practical approach for detection of damage of the connectors than model updating. Another benefit of this method lies in that the environmental effect on the assessment is minimized, which is a key issue in the usual condition assessment or damage detection (Farrar et al. 1997; Xia et al. 2006). This is because the data of the slab and the girders are measured under the similar environmental conditions. As the method is based on the direct comparison of the local response measurements, it can only assess the condition of connectors near the sensors. Hence it is actually a local method. On the other hand, the merit of the model updating method is that it can evaluate the condition of the whole structure including girders, slab and connectors. The drawbacks of the model updating method are that it needs a reliable initial model corresponding to the undamaged state of the structure for comparison, and it is not very sensitive to the damage in the shear connectors. Therefore, whenever possible, it is recommended that the new damage index method proposed in this study should be used for detecting the condition of shear connectors, as it results in more reliable detection.

Composite slab-girder structures are widely used in the construction industry, particularly in bridges and buildings. Their behaviour is significantly affected by the connection between the reinforced concrete slab and the girders. Steel girders are more common than concrete girders, and steel studs

welded in the flange of the girders are usually used as shear connectors. The proposed methods can also be used for condition assessment of the shear connectors or shear links between steel girders and concrete slabs.

ACKNOWLEDGEMENTS

This research was performed with the support of Linkage Project LP0453783 sponsored by Australian Research Council (ARC) and Main Roads Western Australia (MRWA). Special thanks are extended to Robert Scanlon, Adam Lim and Erica Smith. Help from Minhdu Nguyen and Darryl Goedhart of MRWA and Norhisham Bakhary and Zhongyuan Liang of UWA in conducting the field testing is also greatly appreciated.

REFERENCES

ANSYS 8.1. (2004). ANSYS Inc., Southpointe, PA.

Arizumi, Y., and Hamada, S., and Kajita, T. (1981). “Elastic-plastic analysis of composite beams with incomplete interaction by finite element method.” *Computers and Structures*, 14 (5), 453-462.

Australia Standards. (2004a). *Bridge design—Part 5: Concrete*. Standards Australia International Ltd, Sydney, NSW, Australia.

Australia Standards. (2004b). *Bridge design—Part 6: Steel and composite construction*. Standards Australia International Ltd, Sydney, NSW, Australia.

Chen G.D., Yang X.B., Ying X.F. and Nanni A. (2006). “Damage detection of concrete beams using nonlinear features of forced vibration.” *Structural Health Monitoring*, 5(2), 125-141.

Chiewanichakorn, M., Aref, A. J., Chen, S. S. and Ahn, S. (2004). “Effective flange width definition for steel-concrete composite bridge girder.” *Journal of Structural Engineering ASCE*, 130 (12), 2016-2031.

Dilena, M. and Morassi, A. (2003). “A damage analysis of steel-concrete composite beams with dynamic methods: Part II: analytical models and damage detection.” *Journal of Vibration and Control*, 9, 529-565.

Doebling, S.W., Farrar, C.R., Prime, M.B., Shevitz, D.W. (1996). "Damage identification and health monitoring of structural and mechanical systems from changes in their vibration characteristics: a literature review." Los Alamos National Laboratory Report *LA-13070-MS*.

Eom, J. and Nowak, A. S. (2001). "Live Load Distribution for Steel Girder Bridges." *Journal of Bridge Engineering, ASCE*, 6 (6), 489-497.

Ewins, D.J. (2000). *Modal Testing – Theory, Practice and Application*. Baldock (Hertfordshire, UK): Research Studies Press Ltd.

Farrar, C.R., Doebling, S.W., Cornwell, P.J., and Straser, E.G. (1997). "Variability of Modal Parameters Measured on the Alamosa Canyon Bridge." *Proceedings of the 15th International Modal Analysis Conference*, Orlando, Bethel, FL, 257-263.

Hao, H. and Xia, Y. (2002). "Vibration-based Damage Detection of Structures by Genetic Algorithm." *Journal of Computing in Civil Engineering, ASCE*, 16 (3), 222-229.

MATLAB..(2005). *Optimization Toolbox User's Guide*. Version 3, The Mathworks, Inc., Natick, USA.

Morassi, A. and Dilena, M. (2003). "A damage analysis of steel-concrete composite beams with dynamic methods: Part I: Experimental results." *Journal of Vibration and Control*, 9, 507-527.

Oehlers, D. J. (1995). "Design and assessment of shear connectors in composite bridge beams." *Journal of Structural Engineering ASCE*, 121 (2), 214-224

Oehlers, D. J. and Coughlan, C. G. (1986). "The shear stiffness of stud shear connections in composite beams." *Journal of Constructional Steel Research*, 6 (4), 273-284.

Przemieniecki, J. S. (1968). *Theory of Matrix Structural Analysis*, McGraw-Hill, Inc., New York.

Sohn, H., Farrar, C.R., Hemez, F. M., Shunk, D. D., Stinemat, S. W., Nadler, B. R. and Czarnecki, J. J. (2003). "A Review of Structural Health Monitoring Literature form 1996-2001." Los Alamos National Laboratory report *LA-13976-MS*.

Stubbs, N. and Kim J.T. (1996). "Damage localization in structures without baseline modal parameters." *AIAA Journal*, 34(8), 1644-1649.

Swanson, J. A., and Leon, R. T. (2000). "Bolted steel connections: Tests on T-stub components." *Journal of Structural Engineering, ASCE*, 126(1), 50–56.

Swanson, J. A., and Leon, R. T. (2001). "Stiffness modeling of bolted T-stub connection components." *Journal of Structural Engineering, ASCE*, 127 (5), 498-505.

Toksoy, T. and Aktan, A.E. (1994). "Bridge-condition assessment by modal flexibility." *Experimental Mechanics*, 34, 271-278.

Xia, Y., Hao, H. and Deeks, A. (2006a). "Vibration-based Damage Detection of Shear Connectors in Nickol River Bridge and Balla Balla River Bridge, Part III: Results of the Second Testing." School of Civil & Resource Engineering, The University of Western Australia, Australia, *Report No. ST-06-01*.

Xia, Y., Hao, H. and Deeks, A. (2006b). "Dynamic Assessment of Shear Connectors in Slab-Girder Bridges." *Engineering Structures*, in press.

Xia, Y., Hao, H., Zanardo, G., Deeks, A. (2006). "Long Term Vibration Monitoring of A RC Slab: Temperature and Humidity Effect." *Engineering Structures*, 28 (3): 441-452.

Zanardo, G., Hao, H., Xia, Y., and Deeks, A. (2006). "Condition Assessment through Modal Analysis of A Run-on RC Slab Bridge Before and After Strengthening." *Journal of Bridge Engineering, ASCE*, 11 (5), 590-601.

List of figure captions

Figure 1. Beam layout (unit: m)

Figure 2. A pair of shear connectors in the girders (unit: mm)

Figure 3. Top: location of shear connectors in one girder (unit: mm); Middle: mesh of one girder and corresponding connectors in Model 2; Bottom: mesh of one girder and corresponding connectors in Model 1 and Model 3

Figure 4. Measurement grid on the slab

Figure 5. FE model: Model 1

Figure 6. Top: fine model of one span bridge (Model 2), bottom: simplified model of one span bridge (Model 3)

Figure 7. Damage Indicators: Slab (top), Girder (middle) and Shear connector (bottom)

Figure 8. Condition of the shear connectors based on the global method

Figure 9. Model simulation - RDFRFs in the undamaged state (top) and damaged state by removing connectors in the centre of the first span (bottom)

Figure 10. Mean values (top) and standard deviations (bottom) of RDFRFs at A1~A7 in different damage severities

Figure 11. Relative difference of vertical FRFs between the slab and the first girder

Figure 12. Condition of the shear connectors based on the local method

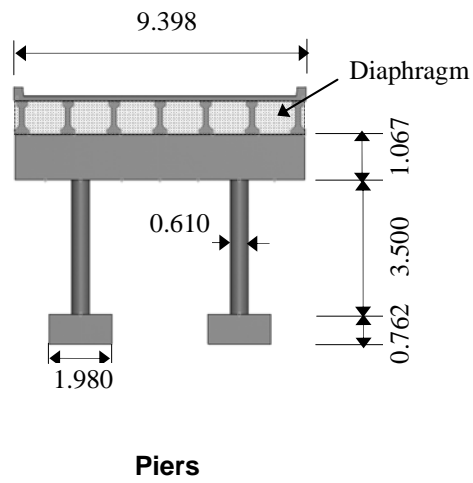
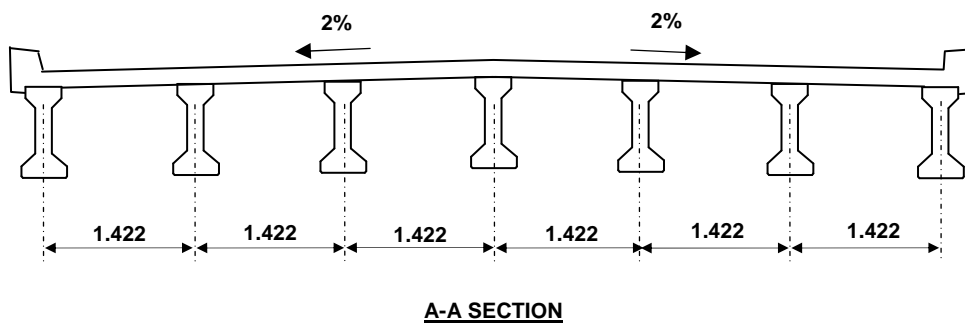
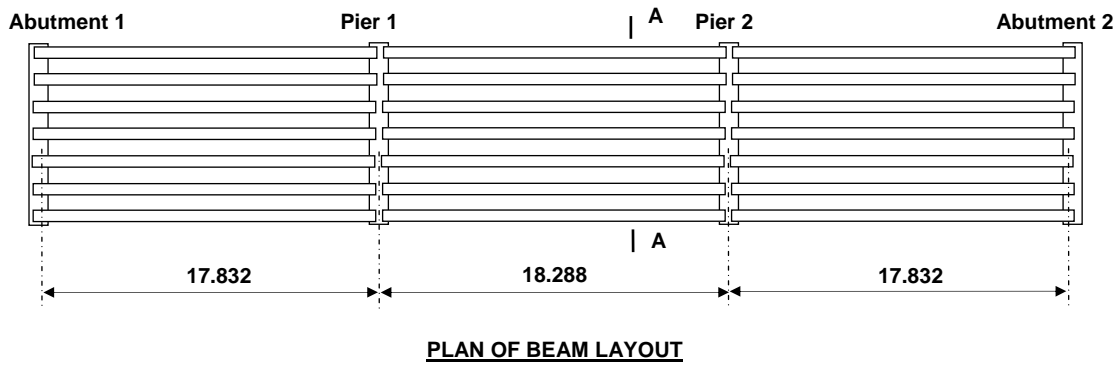


Figure 1. Beam layout (unit: m)

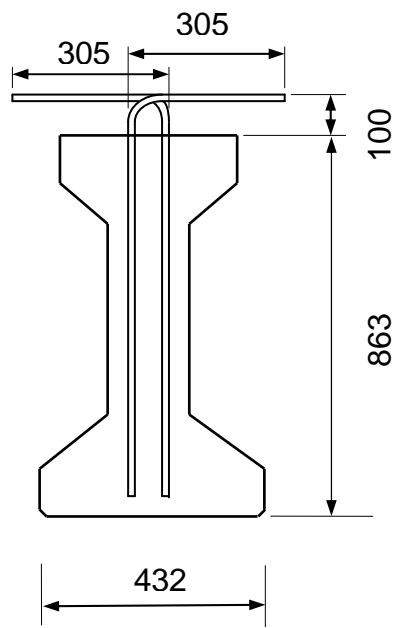


Figure 2. A pair of shear connectors in the girders (unit: mm)

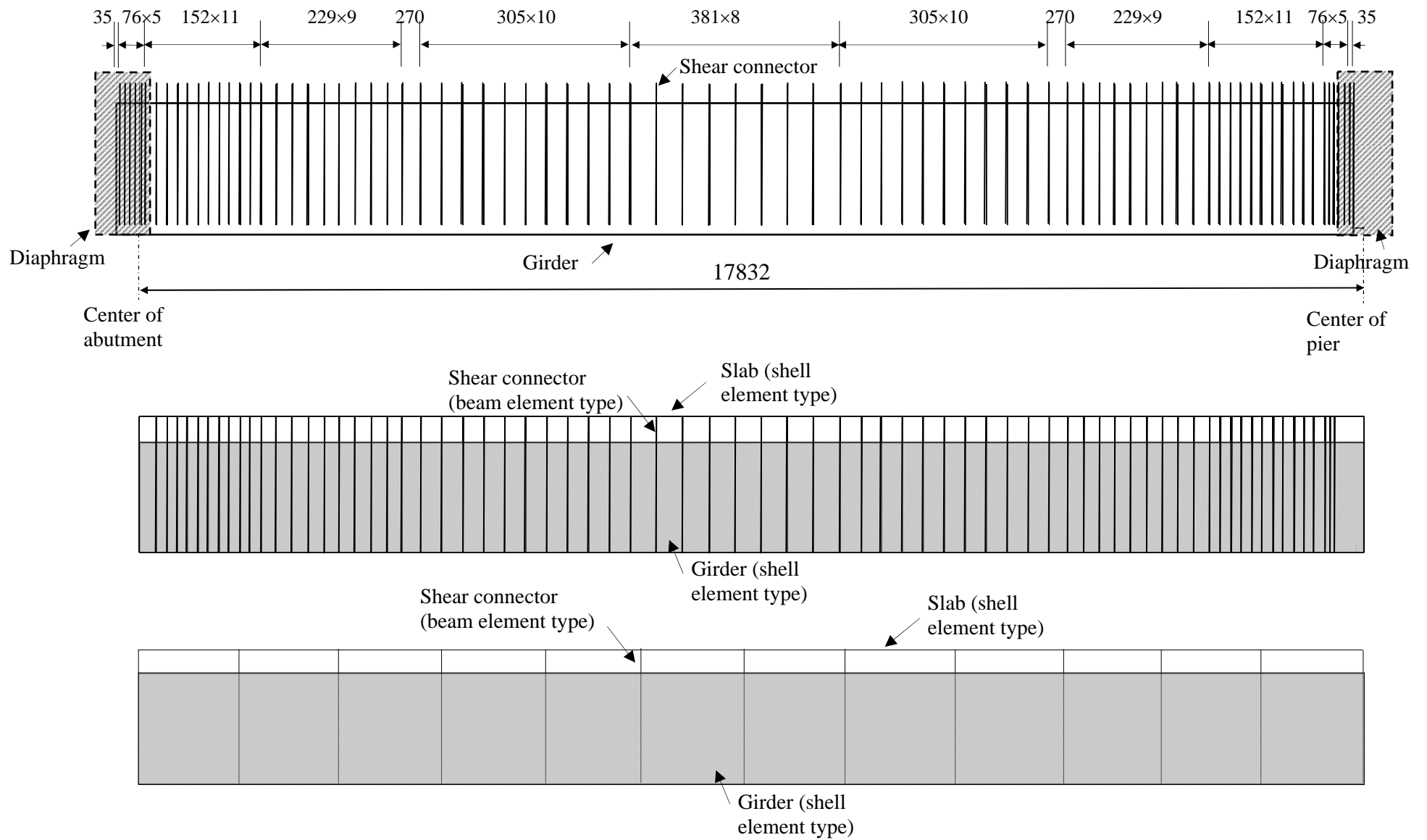


Figure 3. Top: location of shear connectors in one girder (unit: mm); Middle: mesh of one girder and corresponding connectors in Model 2; Bottom: mesh of one girder and corresponding connectors in Model 1 and Model 3

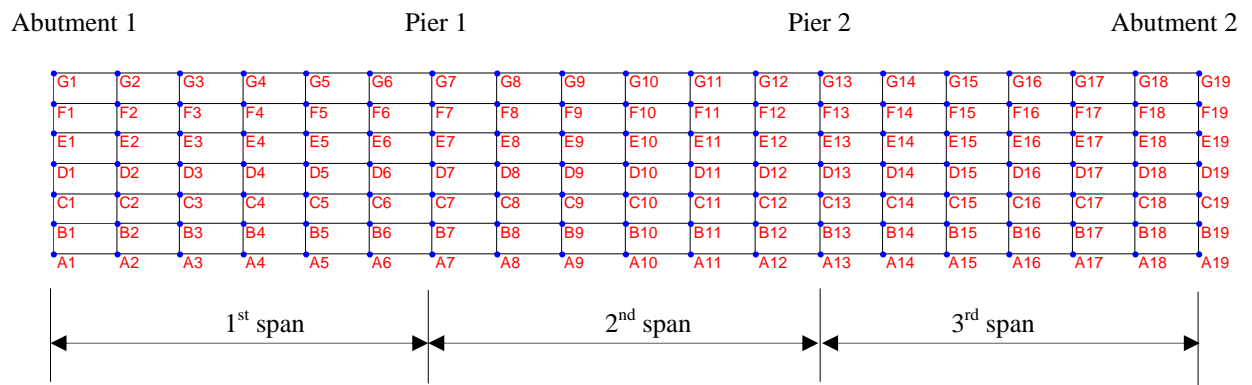


Figure 4. Measurement grid on the slab

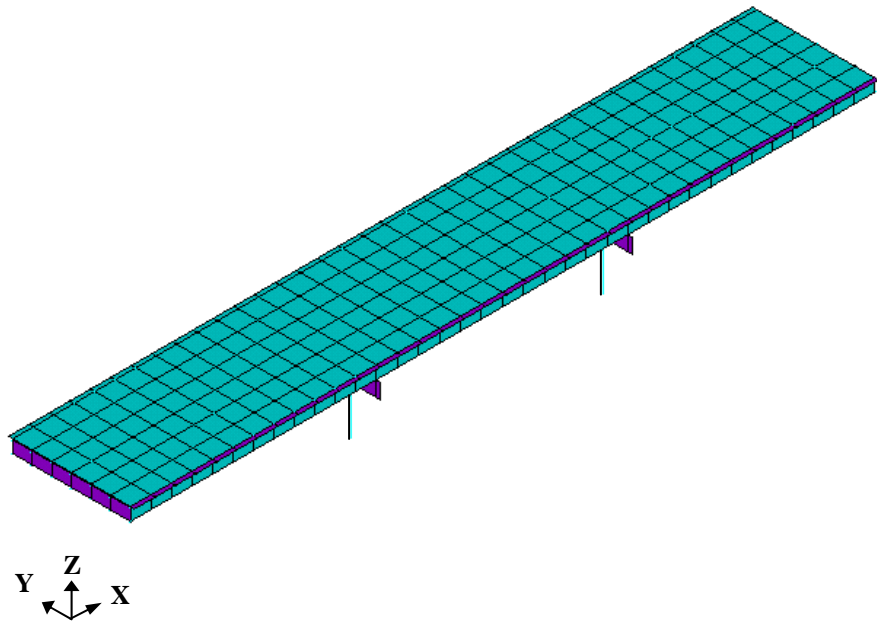


Figure 5. FE model: Model 1

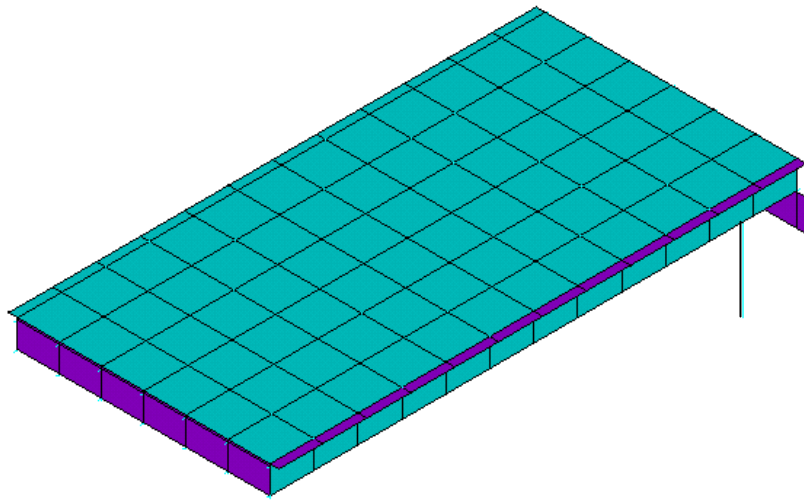
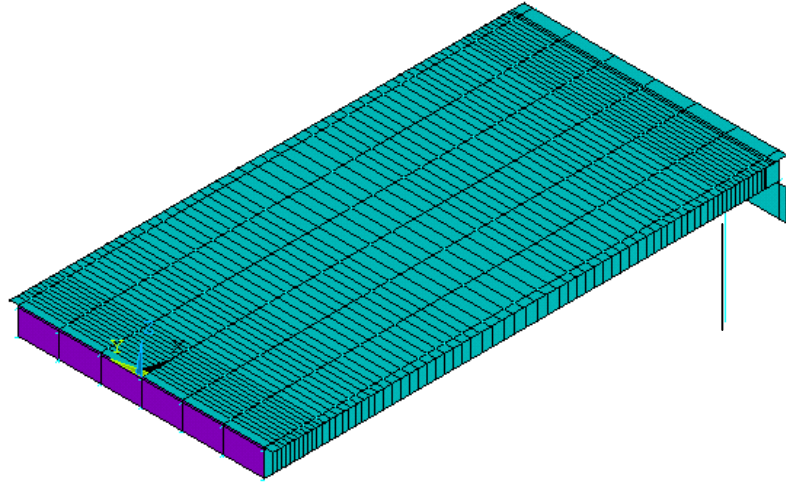
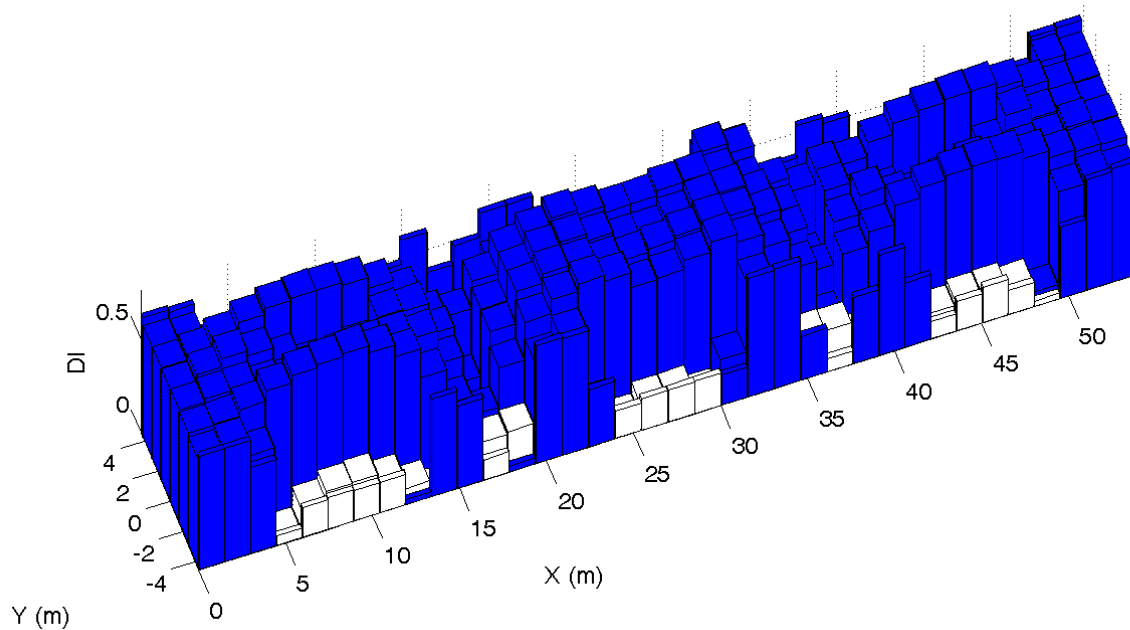
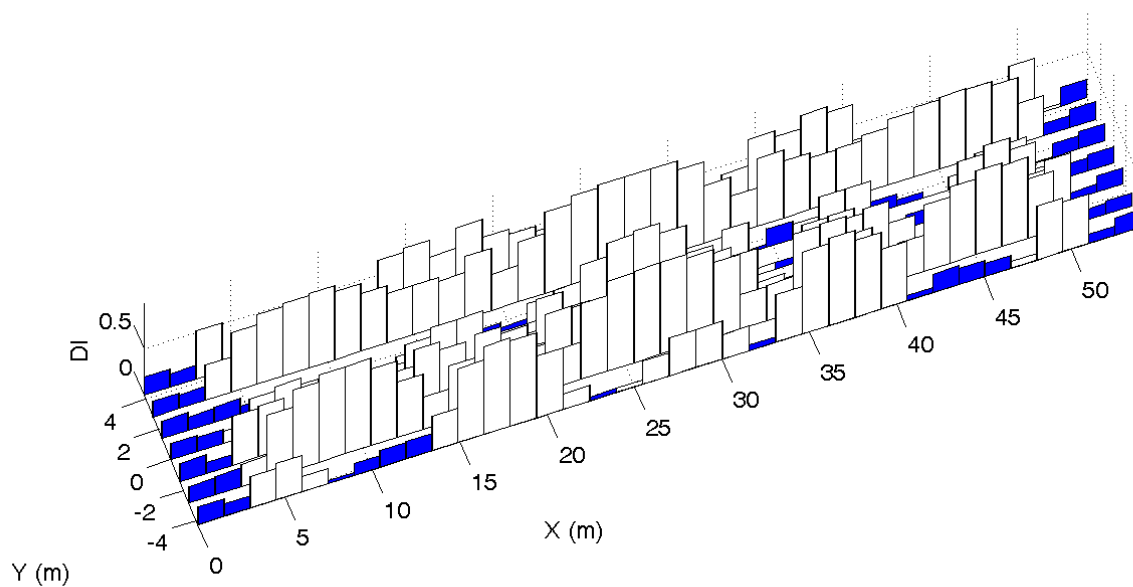


Figure 6. Top: fine model of one span bridge (Model 2), bottom: simplified model of one span bridge (Model 3)

Slab



Girder



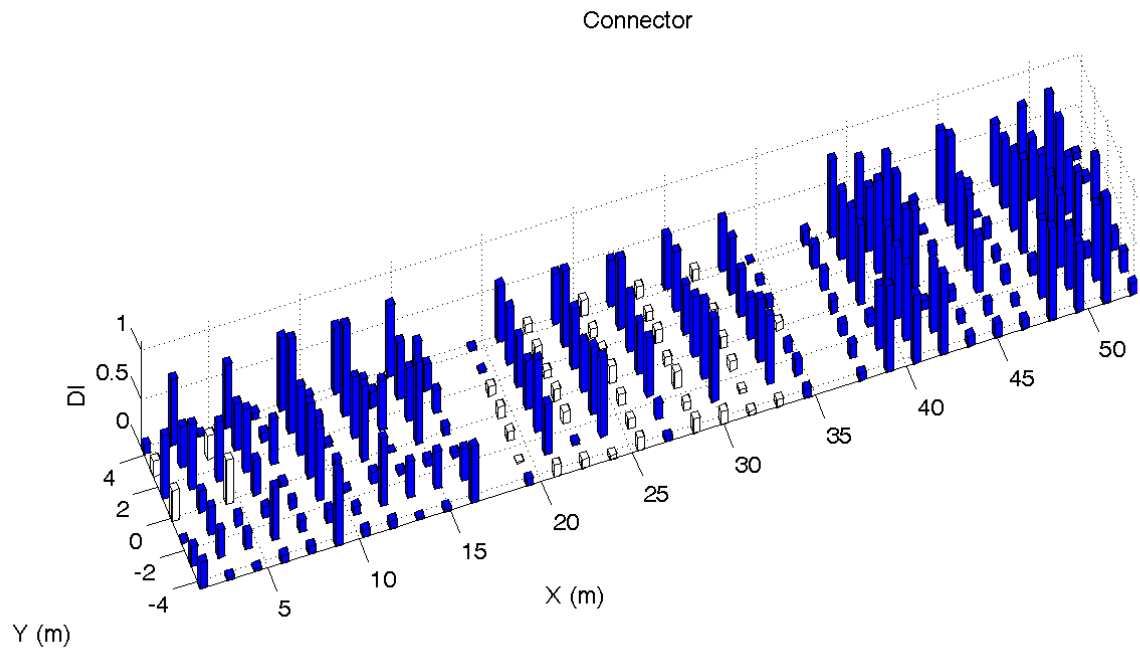


Figure 7. Damage Indicators: Slab (top), Girder (middle) and Shear connector (bottom)

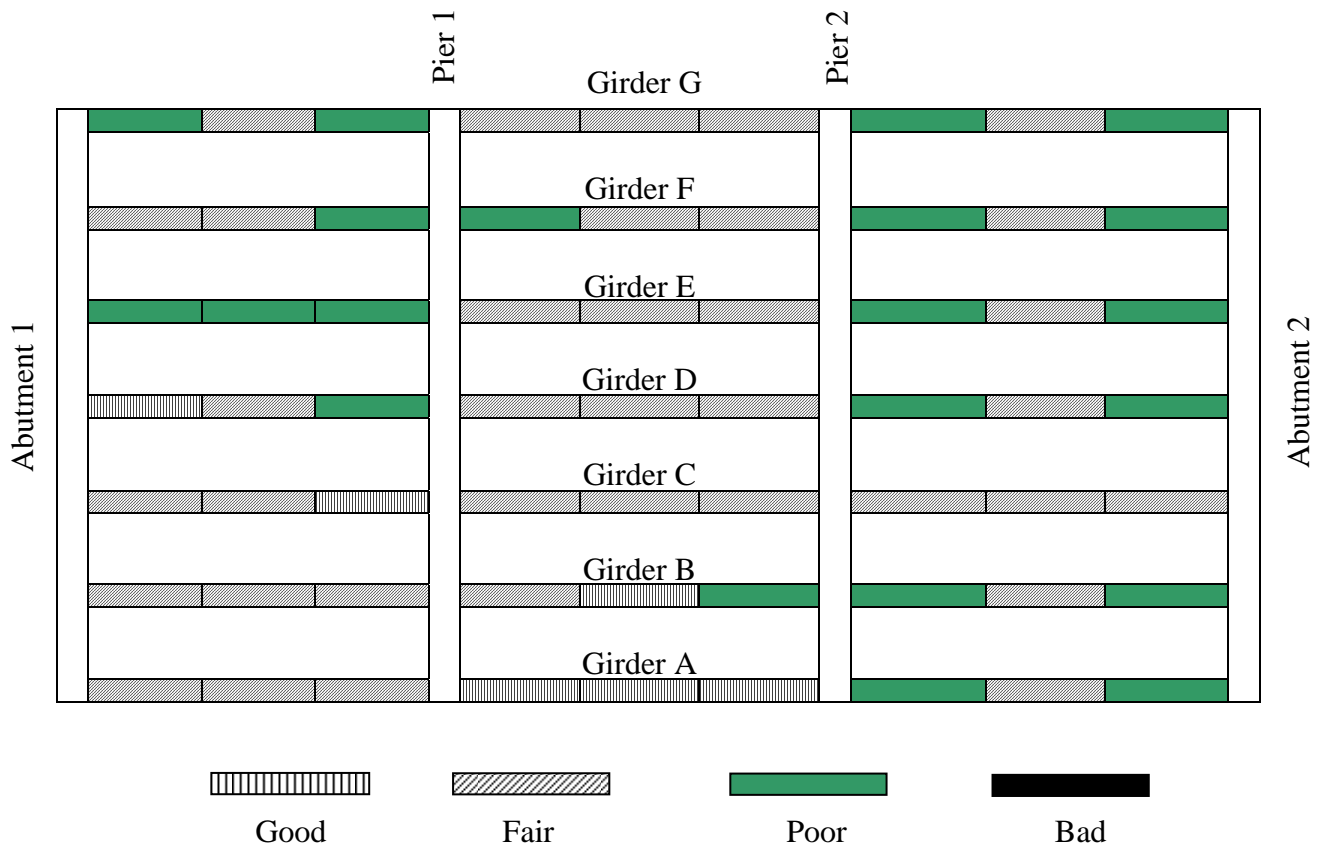


Figure 8. Condition of the shear connectors based on the global method

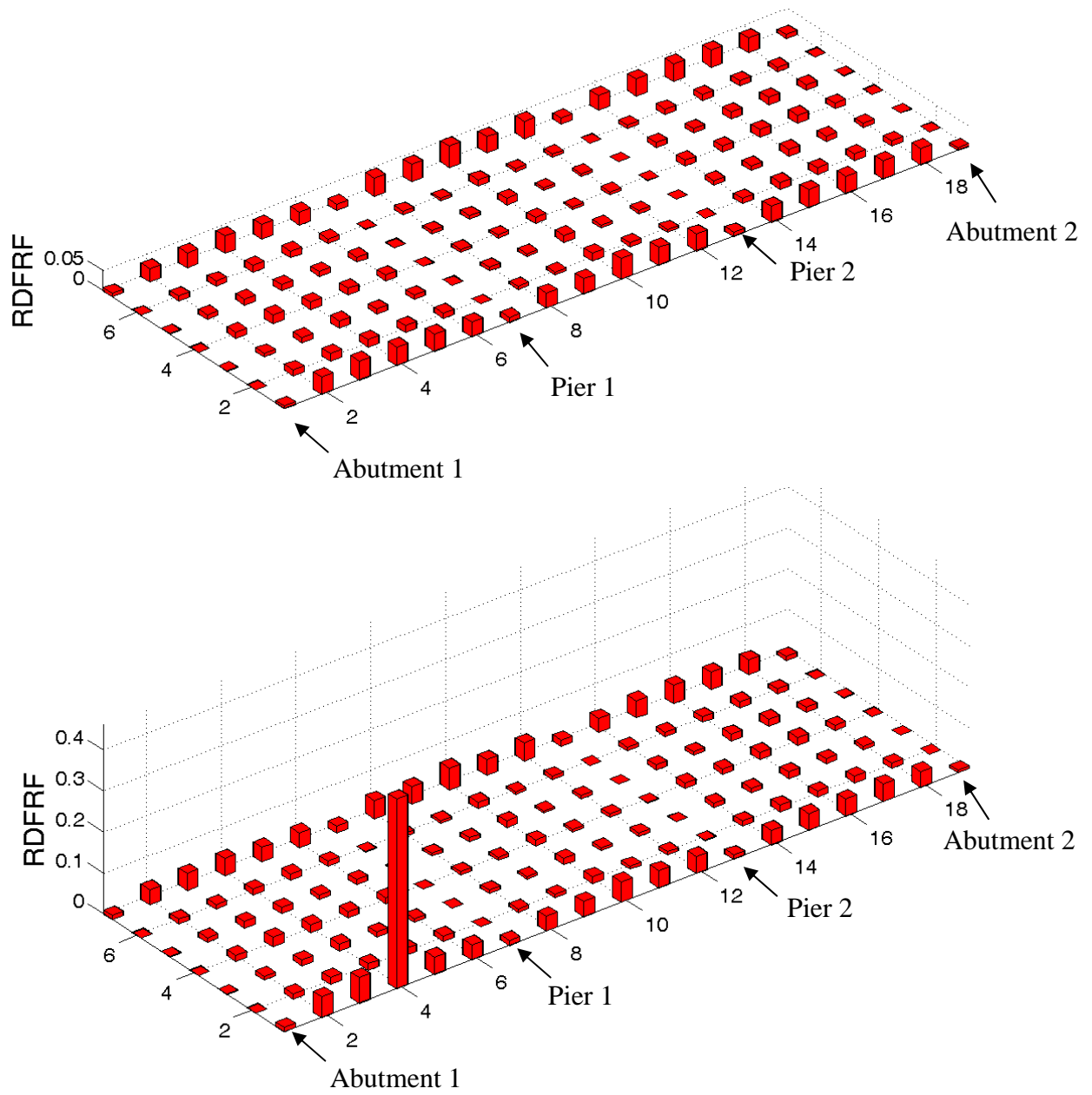


Figure 9. Model simulation - RDFRFs in the undamaged state (top) and damaged state by removing connectors in the centre of the first span (bottom)

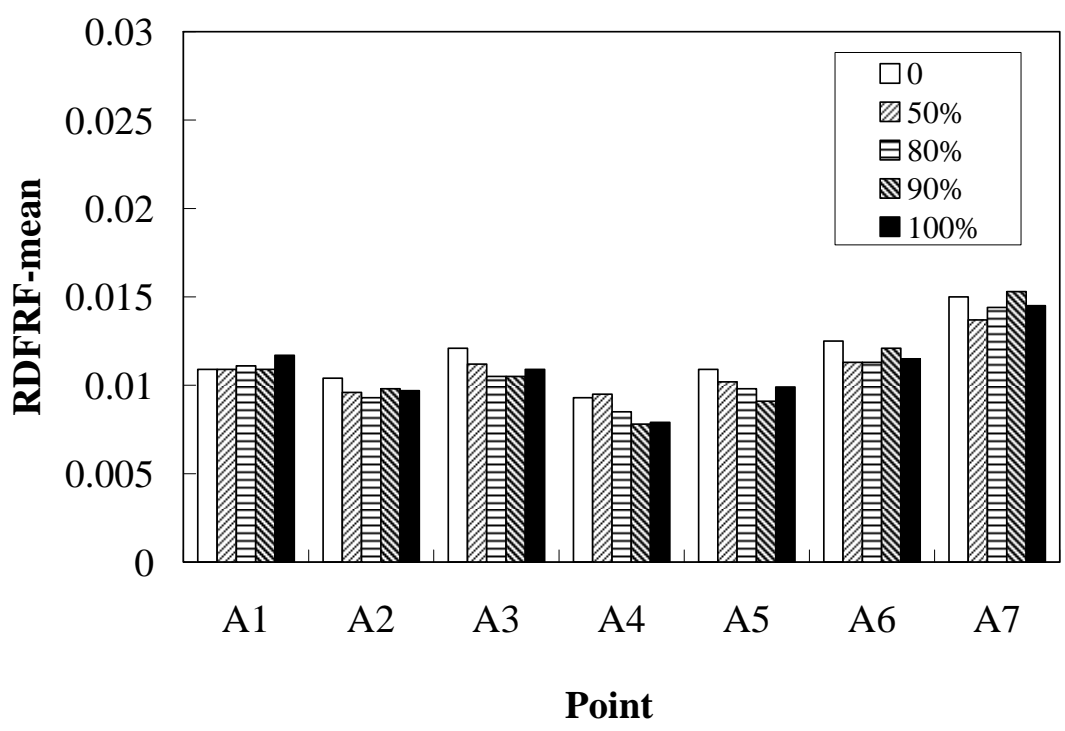
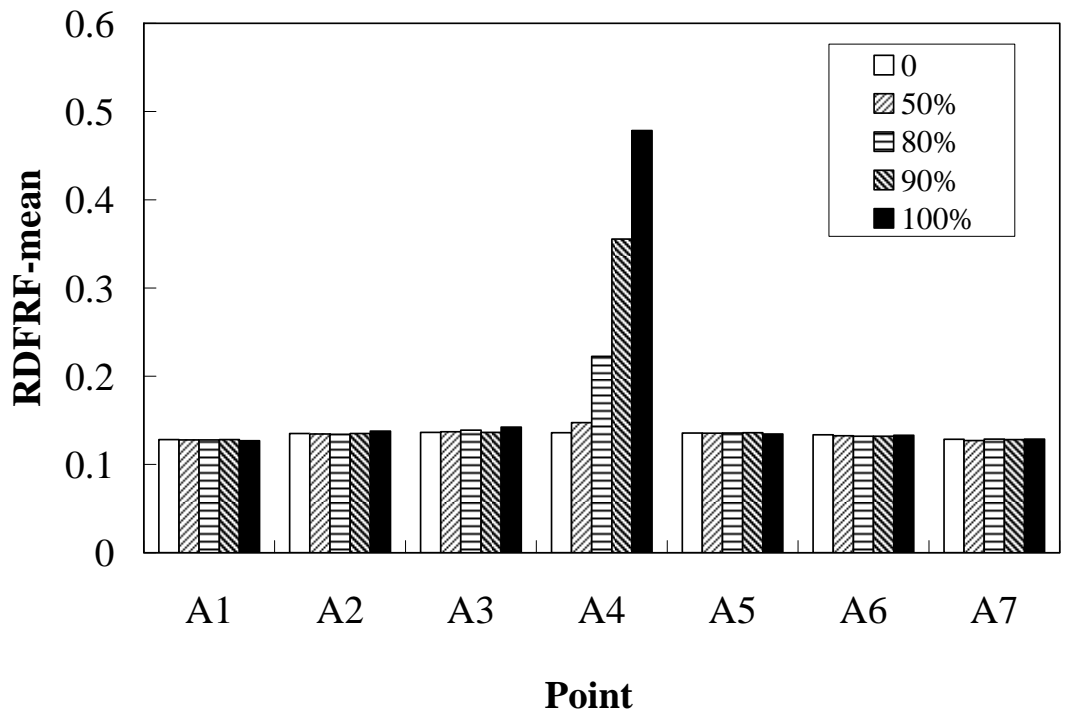


Figure 10. Mean values (top) and standard deviations (bottom) of RDFRFs at A1~A7 in different damage severities

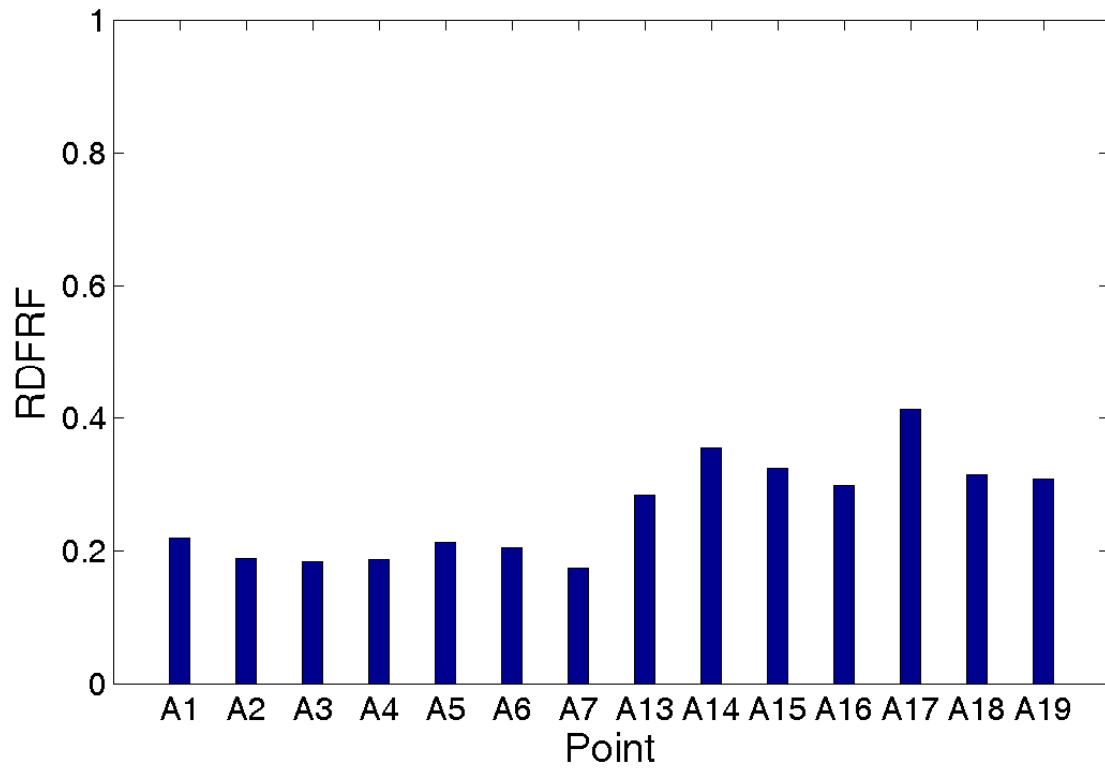


Figure 11. Relative difference of vertical FRFs between the slab and the first girder



Figure 12. Condition of the shear connectors based on the local method

Table 1. Comparison of modal data before and after updating

Mode	Measurement	Before updating			After updating		
	Frequency (Hz)	Frequency (Hz)	Difference (%) ⁺	MAC [*]	Frequency (Hz)	Difference (%) ⁺	MAC [*]
1	6.76	6.26	-7.34	0.93	6.31	-6.61	0.95
2	7.95	7.74	-2.65	0.96	8.02	0.90	0.99
3	10.06	8.71	-13.37	0.71	9.81	-2.46	0.90
4	10.75	12.13	12.84	0.8	11.28	4.97	0.89
5	11.03	9.45	-14.36	0.76	10.77	-2.40	0.80
6	12.64	13.27	4.98	0.85	12.57	-0.58	0.95
7	14.71	17.55	19.29	0.92	15.05	2.33	0.89
8	15.76	18.52	17.49	0.88	15.88	0.74	0.94
9	16.39	18.74	14.35	0.82	16.37	-0.10	0.94
10	20.18	24.91	23.42	0.86	20.33	0.74	0.88
11	29.09	30.16	3.69	0.80	28.56	-1.83	0.92
Averaged value			12.16	0.84		2.02	0.91

⁺ Relative difference of frequency between the model calculation and the measurement;

^{*} Modal Assurance Criterion (MAC) of mode shapes between the model calculation and the measurement